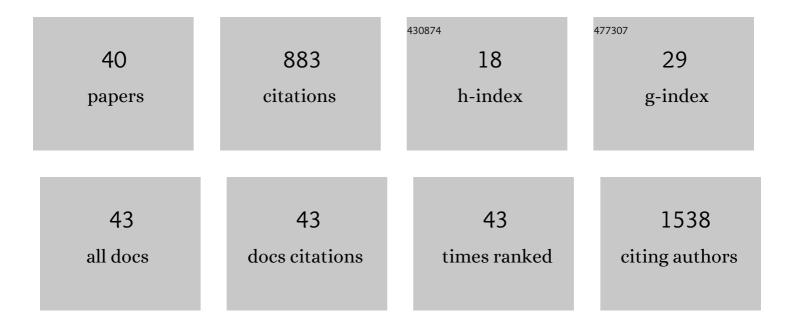
Guillaume Falgayrac

List of Publications by Year in descending order

Source: https://exaly.com/author-pdf/8045745/publications.pdf Version: 2024-02-01



#	Article	IF	CITATIONS
1	Dexamethasone in osteogenic medium strongly induces adipocyte differentiation of mouse bone marrow stromal cells and increases osteoblast differentiation. BMC Cell Biology, 2015, 16, 9.	3.0	77
2	Simultaneous three-dimensional visualization of mineralized and soft skeletal tissues by a novel microCT contrast agent with polyoxometalate structure. Biomaterials, 2018, 159, 1-12.	11.4	70
3	Resolving the internal structure of individual atmospheric aerosol particle by the combination of Atomic Force Microscopy, ESEM–EDX, Raman and ToF–SIMS imaging. Microchemical Journal, 2014, 114, 89-98.	4.5	59
4	Surface Enhanced Raman Spectroscopy for Quantitative Analysis: Results of a Large-Scale European Multi-Instrument Interlaboratory Study. Analytical Chemistry, 2020, 92, 4053-4064.	6.5	50
5	New Method for Raman Investigation of the Orientation of Collagen Fibrils and Crystallites in the Haversian System of Bone. Applied Spectroscopy, 2010, 64, 775-780.	2.2	49
6	Comparability of Raman Spectroscopic Configurations: A Large Scale Cross-Laboratory Study. Analytical Chemistry, 2020, 92, 15745-15756.	6.5	46
7	Tissue-specific mineralization defects in the periodontium of the Hyp mouse model of X-linked hypophosphatemia. Bone, 2017, 103, 334-346.	2.9	38
8	Molecular interactions between zoledronic acid and bone: An in vitro Raman microspectroscopic study. Bone, 2010, 47, 895-904.	2.9	36
9	Chemistry at level of individual aerosol particle using multivariate curve resolution of confocal Raman image. Spectrochimica Acta - Part A: Molecular and Biomolecular Spectroscopy, 2006, 64, 1102-1109.	3.9	32
10	Impaired mineral quality in dentin in X-linked hypophosphatemia. Connective Tissue Research, 2018, 59, 91-96.	2.3	32
11	Raman diagnostic of the reactivity between ZnSO4 and CaCO3 particles in humid air relevant to heterogeneous zinc chemistry in atmosphere. Atmospheric Environment, 2014, 85, 83-91.	4.1	30
12	New Insights on the Composition and the Structure of the Acellular Extrinsic Fiber Cementum by Raman Analysis. PLoS ONE, 2016, 11, e0167316.	2.5	29
13	Dual-energy computed-tomography-based discrimination between basic calcium phosphate and calcium pyrophosphate crystal deposition <i>in vivo</i> . Therapeutic Advances in Musculoskeletal Disease, 2020, 12, 1759720X2093606.	2.7	25
14	Heterogeneous chemistry between PbSO4 and calcite microparticles using Raman microimaging. Spectrochimica Acta - Part A: Molecular and Biomolecular Spectroscopy, 2006, 64, 1095-1101.	3.9	23
15	Region specific Raman spectroscopy analysis of the femoral head reveals that trabecular bone is unlikely to contribute to non-traumatic osteonecrosis. Scientific Reports, 2017, 7, 97.	3.3	23
16	Unraveling the compromised biomechanical performance of type 2 diabetes- and Roux-en-Y gastric bypass bone by linking mechanical-structural and physico-chemical properties. Scientific Reports, 2018, 8, 5881.	3.3	23
17	Doses effects of zoledronic acid on mineral apatite and collagen quality of newly-formed bone in the rat's calvaria defect. Bone, 2016, 89, 32-39.	2.9	22
18	Defective Mineralization in X-Linked Hypophosphatemia Dental Pulp Cell Cultures. Journal of Dental Research, 2018, 97, 184-191.	5.2	22

Guillaume Falgayrac

#	Article	IF	CITATIONS
19	Multi-energy photon-counting computed tomography versus other clinical imaging techniques for the identification of articular calcium crystal deposition. Rheumatology, 2021, 60, 2483-2485.	1.9	20
20	Comparison of Two-Dimensional Fast Raman Imaging versus Point-by-Point Acquisition Mode for Human Bone Characterization. Analytical Chemistry, 2012, 84, 9116-9123.	6.5	17
21	Heterogeneous microchemistry between CdSO4 and CaCO3 particles under humidity and liquid water. Journal of Hazardous Materials, 2013, 248-249, 415-423.	12.4	17
22	Molecular alterations of bone quality in sequesters of bisphosphonates-related osteonecrosis of the jaws. Osteoporosis International, 2014, 25, 747-756.	3.1	17
23	Bone Samples Extracted from Embalmed Subjects Are Not Appropriate for the Assessment of Bone Quality at the Molecular Level Using Raman Spectroscopy. Analytical Chemistry, 2016, 88, 2777-2783.	6.5	16
24	Mandibular bone is protected against microarchitectural alterations and bone marrow adipose conversion in ovariectomized rats. Bone, 2019, 127, 343-352.	2.9	16
25	A Preliminary Investigation into the Effects of X-Ray Radiation on Superficial Cranial Vascularization. Calcified Tissue International, 2009, 84, 379-387.	3.1	13
26	No anti-angiogenic effect of clinical dosing regimens of a single zoledronic acid injection in an experimental bone healing site. Bone, 2010, 46, 643-648.	2.9	13
27	Rate constants for the decomposition of 2-butoxy radicals and their reaction with NO and O2. Physical Chemistry Chemical Physics, 2004, 6, 4127.	2.8	11
28	Bone matrix quality in paired iliac bone biopsies from postmenopausal women treated for 12Âmonths with strontium ranelate or alendronate. Bone, 2021, 153, 116107.	2.9	10
29	Particle–Particle Chemistry between Micrometer-Sized PbSO ₄ and CaCO ₃ Particles in Turbulent Flow Initiated by Liquid Water. Journal of Physical Chemistry A, 2012, 116, 7386-7396.	2.5	9
30	Mica Dust and Pneumoconiosis. Journal of Occupational and Environmental Medicine, 2013, 55, 1469-1474.	1.7	9
31	Noninvasive molecular identification of particulate matter in lungs by Raman microspectrometry. Journal of Raman Spectroscopy, 2011, 42, 1484-1487.	2.5	8
32	Subchondral involvement in osteonecrosis of the femoral head: insight on local composition, microstructure and vascularization. Osteoarthritis and Cartilage, 2022, 30, 1103-1115.	1.3	7
33	Critical aspects of Raman spectroscopy as a tool for postmortem interval estimation. Talanta, 2022, 249, 123589.	5.5	7
34	Effects of high dose of zoledronic acid on superficial vascular network of membranous bone sites: an intravital study on rat calvarium. Osteoporosis International, 2010, 21, 1919-1925.	3.1	2
35	Laser preconditioning on cranial bone site: Analysis of morphological vascular parameters. Lasers in Surgery and Medicine, 2010, 42, 791-797.	2.1	2
36	Influence of collecting substrate on the Raman imaging of micron-sized particles. Analytica Chimica Acta, 2018, 1014, 41-49.	5.4	1

Guillaume Falgayrac

#	Article	IF	CITATIONS
37	Severity Level and Duration of Energy Deficit in Mice Affect Bone Phenotype and Bone Marrow Stromal Cell Differentiation Capacity. Frontiers in Endocrinology, 0, 13, .	3.5	1
38	Shortâ€ŧerm highâ€dose zoledronic acid enhances crystallinity in mandibular alveolar bone in rats. European Journal of Oral Sciences, 2020, 128, 284-291.	1.5	0
39	Bisphosphonate influence on bone quality at molecular level: study of human jaw bone sequesters by Raman microspectroscopy. Bone Abstracts, 0, , .	0.0	О
40	Preliminary Protocol to Identify Parturitions Lines in Acellular Cementum. , 2022, , 234-248.		0